ISSN 1070-3284, Russian Journal of Coordination Chemistry, 2020, Vol. 46, No. 2, pp. 145–151. © Pleiades Publishing, Ltd., 2020.

Nickel(II) Complexes Derived from Bis-Schiff Bases: Synthesis, Crystal Structures, and Antimicrobial Activity

L. W. Xue[a, b, *], Y. J. Han[a], and X. Q. Luo[a]

[a] *School of Chemical and Environmental Engineering, Pingdingshan University, Pingdingshan Henan, 467000 P.R. China*

[b] *Henan Key Laboratory of Research for Central Plains Ancient Ceramics, Pingdingshan University, Pingdingshan Henan, 467000 P.R. China*

**e-mail: pdsuchemistry@163.com*

Received May 1, 2019; revised June 12, 2019; accepted August 14, 2019

Abstract—Nickel(II) complexes derived from the bis-Schiff bases *N,N'*-bis(5-methylsalicylidene)-1,2-diaminocyclohexane (H_2L^a), *N,N'*-bis(5-methylsalicylidene)-1,2-diaminoethane (H_2L^b) and *N,N'*-bis(3,5-difluorosalicylidene)-1,2-diaminoethane (H_2L^c), respectively, have been prepared and characterized by elemental analyses, IR, UV–Vis and single crystal XRD (CIF files CCDC nos. 1912770 (**I**), 1912771 (**II**), and 1912772 (**III**)). The bis-Schiff base ligands coordinate to the nickel atoms through phenolate O and imine N atoms. Each metal atom in the complexes is in square planar coordination. The effects of the complexes on the antimicrobial activity against *Staphylococcus aureus*, *Escherichia coli*, and *Candida albicans* were studied, which indicate that the fluoro-substituted groups are essential for the biological process.

Keywords: bis-Schiff-bases, crystal structure, antimicrobial activity, intermolecular hydrogen bonds, powder and single crystal XRD

DOI: 10.1134/S1070328420020098

INTRODUCTION

Schiff bases are a kind of important ligands in coordination chemistry [1–3]. In recent years, metal complexes of Schiff bases have attracted much attention due to their versatile biological activity, such as antifungal antibacterial and antitumor [4–6]. It has been shown that the Schiff base complexes derived from salicylaldehyde and its derivatives with primary amines, bearing the N_2O, N_2S, NO_2 or NSO donor sets have interesting biological activity [7–10]. Recent research indicates that the halide-substituent groups in aromatic rings of Schiff bases can severely increase the antimicrobial activity [11]. In the present paper, the preparation, characterization and antimicrobial activity of three nickel(II) complexes, [NiL^a] (**I**), [NiL^b] · CH_3OH (**II**) and [NiL^c] (**III**), with bis-Schiff bases *N,N'*-bis(5-methylsalicylidene)-1,2-diaminocyclohexane (H_2L^a), *N,N'*-bis(5-methylsalicylidene)-1,2-diaminoethane (H_2L^b) and *N,N'*-bis(3,5-difluorosalicylidene)-1,2-diaminoethane (H_2L^c), respectively, are reported.

EXPERIMENTAL

Material and methods. 5-Methylsalicylaldehyde, 3,5-difluorosalicylaldehyde, 1,2-diaminocyclohexane, and 1,2-diaminoethane with analytical reagent grade were purchased from Fluka. Other reagents and solvents were analytical grade and used without further purification. Elemental (C, H, and N) analyses were made on a PerkinElmer Model 240B automatic analyser. Infrared (IR) spectra were recorded on an IR-408 Shimadzu 568 spectrophotometer. UV–Vis spectra were recorded on a Lambdar 35 spectrometer. X-ray diffraction was carried out on a Bruker SMART 1000 CCD area diffractometer. The powder X-ray diffraction (XRD) spectra were recorded in a 2θ range of 2°–50° using a Bruker D8 Advance detector under ambient conditions.

Synthesis of I. 5-Methylsalicylaldehyde (0.272 g, 2 mmol) and 1,2-diaminocyclohexane (0.114 g, 1 mmol) were reacted in methanol (30 mL) at ambient temperature for 1 h. Then, nickel chloride hexahydrate (0.238 g, 1 mmol) dissolved in methanol (5 mL) were added dropwise to the solution. The mixture was stirred for 30 min at ambient temperature. The filtered solution was allowed to slow evaporate in an uncapped vial. Several days later, block crystals of complex **I** were obtained. The yield was 183 mg (45%).

For $C_{22}H_{24}N_2O_2Ni$			
Anal. calcd., %:	C, 64.90	H, 5.94	N, 6.88
Found, %	C, 64.75	H, 6.08	N, 6.77

Selected IR data (ν, cm^{-1}): 1626 s, ν(C=N). UV–Vis data in methanol (λ_{max}, nm (ε, L mol^{-1} cm^{-1})): 245 (15320); 256 (14565); 318 (3633); 410 (2720); 578 (550).

Synthesis of II. 5-Methylsalicylaldehyde (0.272 g, 2 mmol) and 1,2-diaminoethane (0.060 g, 1 mmol) were reacted in methanol (30 mL) at ambient temperature for 1 h. Then, nickel chloride hexahydrate (0.238 g, 1 mmol) dissolved in methanol (5 mL) were added dropwise to the solution. The mixture was stirred for 30 min at ambient temperature. The filtered solution was allowed to slow evaporate in an uncapped vial. Several days later, block crystals of complex **II** were obtained. The yield was 212 mg (55%).

For $C_{19}H_{22}N_2O_3Ni$

Anal. calcd., %	C, 59.26	H, 5.76	N, 7.27
Found, %	C, 59.41	H, 5.85	N, 7.18

Selected IR data (ν, cm^{-1}): 1627 s, ν(C=N). UV–Vis data in methanol (λ_{max}, nm (ε, L mol^{-1} cm^{-1})): 245, 16130; 255, 14723; 330, 3571; 410, 2930; 575, 530.

Synthesis of III. 3,5-Difluorosalicylaldehyde (0.316 g, 2 mmol) and 1,2-diaminoethane (0.060 g, 1 mmol) were reacted in methanol (30 mL) at ambient temperature for 1 h. Then, nickel chloride hexahydrate (0.238 g, 1 mmol) dissolved in methanol (5 mL) were added dropwise to the solution. The mixture was stirred for 30 min at ambient temperature. The filtered solution was allowed to slow evaporate in an uncapped vial. Several days later, block crystals of complex **III** were obtained. The yield was 165 mg (42%).

For $C_{16}H_{10}N_2O_2F_4Ni$

Anal. calcd., %	C, 48.41	H, 2.54	N, 7.06
Found, %	C, 48.55	H, 2.43	N, 7.13

Selected IR data (ν, cm^{-1}): 1627 s, ν(C=N). UV–Vis data in methanol (λ_{max}, nm (ε, L mol^{-1} cm^{-1})): 237, 18320; 250, 16160; 340, 4770; 403, 3835; 580, 610.

X-ray diffraction. Data were collected from selected crystals mounted on glass fibers. The data for the three complexes were processed with SAINT [12] and corrected for absorption using SADABS [13]. Multi-scan absorption corrections were applied with ψ-scans [14]. The structures were solved by direct methods using the program SHELXS-97 and refined by full-matrix least-squares techniques on F^2 using anisotropic displacement parameters [15]. Hydrogen atoms were placed at the calculated positions. Idealized H atoms were refined with isotropic displacement parameters set to 1.2 (1.5 for methyl and hydroxyl groups) times the equivalent isotropic U values of the parent carbon atoms. The crystallographic data for the complexes are listed Table 1.

Supplementary material has been deposited with the Cambridge Crystallographic Data Centre (nos. 1912770 (**I**), 1912771 (**II**) and 1912772 (**III**); deposit@ccdc.cam.ac.uk or http://www.ccdc.cam.ac.uk).

RESULTS AND DISCUSSION

The three Schiff bases were readily prepared by the condensation of 1 : 2 molar ratio of 1,2-diaminocyclohexane with 5-methylsalicylaldehyde, 1,2-diaminoethane with 5-methylsalicylaldehyde, and 1,2-diaminoethane with 3,5-difluorosalicylaldehyde, respectively, in methanol at ambient temperature. The Schiff bases were not isolated and used directly to the synthesis of the complexes with nickel chloride hexahydrate. The complexes are very stable at room temperature in the solid state and soluble in common organic solvents, such as methanol, ethanol, chloroform, and acetonitrile. The results of the elemental analyses are in accord with the composition suggested for the complexes.

The molecular structures of the three complexes are shown in Fig. 1. Selected bond distances and angles are listed in Table 2. Complex **II** contains a mononuclear [NiL^b] complex molecule and a methanol molecule of crystallization. Complex **III** possesses a crystallographic two-fold rotation axis symmetry. The nickel complex molecules are similar to each other with the Ni atoms in square planar geometry. The Ni atoms in the complexes are coordinated by two phenolate oxygen atoms and two imino nitrogen atoms. The Ni–O and Ni–N atoms in the three complexes are similar to each other, and comparable to those observed in similar nickel(II) complexes with Schiff bases [16–18].

In the crystal structure of complex **I**, two molecules are linked through intermolecular C–H···O hydrogen bonds (Table 3) to form a dimeric structure (Fig. 2a). In the crystal structure of complex **II**, the methanol molecules are linked to the complex molecules through O–H···O hydrogen bonds, and the complex molecules are linked through intermolecular C–H···O hydrogen bonds (Table 3) to form a dimeric structure (Fig. 2b). In the crystal structure of complex **III**, the complex molecules are linked through intermolecular C–H···F hydrogen bonds (Table 3) to form a network (Fig. 2c).

The experimental powder XRD patterns of the bulk products of complexes **I**, **II** and **III** are in good agreement with the simulated XRD patterns from single crystal XRD, indicating purity of the bulk samples (Fig. 3). The simulated patterns of the complexes were calculated from the single crystal structural data using the PCW software.

The IR spectra of the free Schiff bases contain strong C–O absorption bands in the region 1240–1255 cm^{-1}. The bands disappeared on complexation,

Table 1. Crystallographic data and experimental details for complexes **I**–**III**

Parameter	Value		
	I	**II**	**III**
Habit; color	Block; red	Block; red	Block; red
Fw	407.1	385.10	396.97
Temperature, K	298(2)	298(2)	298(2)
Crystal size, mm	0.15 × 0.15 × 0.13	0.23 × 0.22 × 0.20	0.20 × 0.15 × 0.15
Radiation (λ, Å)	MoK_α (0.71073)	MoK_α (0.71073)	MoK_α (0.71073)
Crystal system	Monoclinic	Triclinic	Monoclinic
Space group	$P2_1/c$	$P\bar{1}$	$C2/c$
Unit cell dimensions:			
a, Å	13.4159(15)	6.7105(11)	26.0251(18)
b, Å	13.7566(13)	10.6650(13)	8.6780(17)
c, Å	10.4817(9)	12.626(2)	6.7683(11)
α, deg	90	87.190(1)	90
β, deg	102.6130(10)	88.876(1)	100.787(1)
γ, deg	90	89.777(1)	90
V, Å^3	1887.8(3)	902.3(2)	1501.6(4)
Z	4	2	4
ρ_{calcd}, g cm^{-3}	1.433	1.417	1.756
F(000)	856	404	800
Absorption coefficient, mm^{-1}	1.047	1.095	1.351
θ Range for data collection, deg	2.15–25.50	1.62–25.50	1.59–25.49
Reflections collected	10290	5392	15573
Independent reflections (R_{int})	3494 (0.1118)	3345	1404 (0.0346)
Reflections with $I > 2\sigma(I)$	1879	2240	1097
Data/parameters	3494/246	3345/230	1404/114
Restraints	0	0	0
Goodness-of-fit on F^2	0.966	1.039	1.065
Final *R* indices ($I > 2\sigma(I)$)	$R_1 = 0.0466$, $wR_2 = 0.0845$	$R_1 = 0.0558$, $wR_2 = 0.1186$	$R_1 = 0.0257$, $wR_2 = 0.0697$
R indices (all data)	$R_1 = 0.1311$, $wR_2 = 0.1113$	$R_1 = 0.0946$, $wR_2 = 0.1393$	$R_1 = 0.0361$, $wR_2 = 0.0770$
Largest difference peak and hole, e Å^{-3}	0.347 and –0.525	0.390 and –0.347	0.200 and –0.185

and new C–O absorption bands appeared in the region 1080–1105 cm^{-1} in the spectra of the complexes, indicating that the Schiff bases coordinate to the nickel atoms through deprotonated form. The infrared spectra of the complexes display intense absorption bands at 1627 cm^{-1}, which can be assigned to the C=N stretching frequencies of the Schiff base ligands, whereas for the free Schiff bases the corresponding absorption bands are observed at higher wave numbers (1635–1640 cm^{-1}). The shift of these bands on complexation towards lower wave number indicates coordination of the imine nitrogen to the nickel center [19].

The UV–Vis spectra of the complexes were recorded in methanol solution. The complexes show two charge transfer bands at about 255 and 330 nm, which are attributed to π–π* and *n*–π* transitions within the Schiff base ligands. The weak absorption bands at about 580 nm can be assigned to the *d*–*d* transitions.

Qualitative determination of antimicrobial activity was done using the disk diffusion method [20, 21]. The

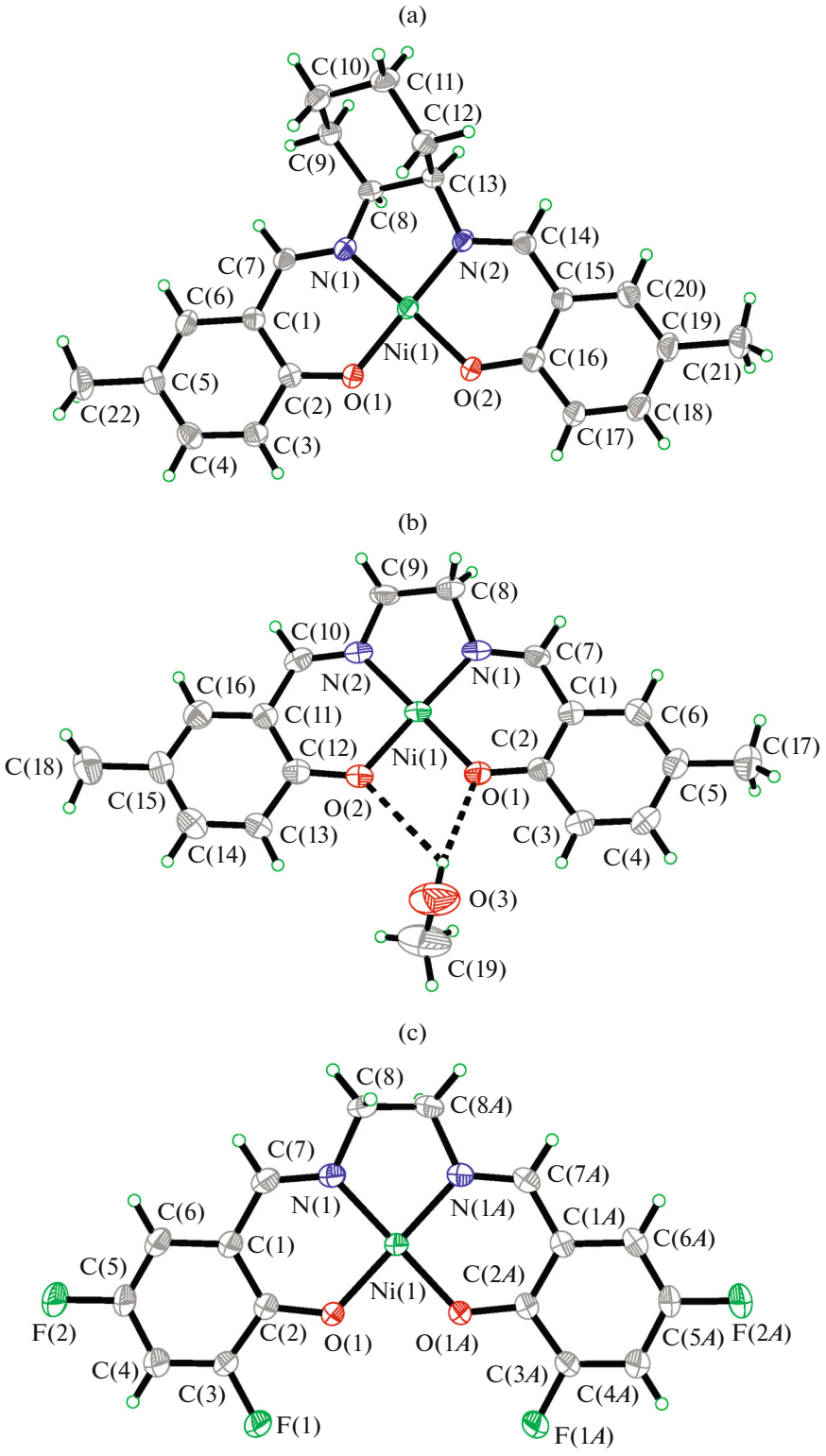

Fig. 1. Molecular structure of complexes **I** (a), **II** (b), **III** (c) with 30% probability thermal ellipsoids.

results are summarized in Table 4. A comparative study of minimum inhibitory concentration (MIC) values of the Schiff bases and the complexes indicate that the nickel complexes have higher activity than the free Schiff bases. Generally, this is caused by the greater lipophilic nature of the complexes than the

Table 2. Selected bond distances (Å) and angles (deg) for I–**III***

Bond	*d*, Å	Bond	*d*, Å
		I	
Ni(1)–O(1)	1.842(3)	Ni(1)–O(2)	1.851(3)
Ni(1)–N(1)	1.860(3)	Ni(1)–N(2)	1.835(3)
		II	
Ni(1)–O(1)	1.849(3)	Ni(1)–O(2)	1.846(3)
Ni(1)–N(1)	1.833(4)	Ni(1)–N(2)	1.847(4)
		III	
Ni(1)–O(1)	1.8457(13)	Ni(1)–N(1)	1.8493(17)
Angle	ω, deg	Angle	ω, deg
		I	
N(2)Ni(1)O(1)	177.44(14)	N(2)Ni(1)O(2)	94.72(14)
O(1)Ni(1)O(2)	84.46(12)	N(2)Ni(1)N(1)	85.86(16)
O(1)Ni(1)N(1)	95.15(15)	O(2)Ni(1)N(1)	175.50(14)
		II	
N(1)Ni(1)O(2)	177.94(15)	N(1)Ni(1)N(2)	86.35(18)
O(2)Ni(1)N(2)	94.89(17)	N(1)Ni(1)O(1)	94.57(16)
O(2)Ni(1)O(1)	84.21(14)	N(2)Ni(1)O(1)	179.02(16)
		III	
O(1)Ni(1)O(1*A*)	85.47(8)	O(1)Ni(1)N(1*A*)	177.63(7)
O(1)Ni(1)N(1)	94.37(7)	N(1)Ni(1)N(1*A*)	85.89(10)

* Symmetry code for *A*: $-x$, $1-y$, $-z$ (**III**).

Table 3. Geometric parameters of hydrogen bond for complexes **I**–**III***

D–H···A	Distance, Å			Angle D–H···A, deg
	D–H	H···A	D···A	
		I		
C(8)–H(8)···O(1)$^{\#1}$	0.98	2.37(2)	3.259(3)	150(5)
		II		
O(3)–H(3*A*)···O(1)	0.82	2.08(3)	2.890(4)	169(5)
C(9)–H(9*A*)···O(1)$^{\#2}$	0.97	2.54(3)	3.363(4)	143(5)
		III		
C(4)–H(4)···F(2)$^{\#3}$	0.93	2.54(2)	3.465(3)	172(4)
C(8)–H(8*B*)···F(1)$^{\#4}$	0.97	2.31(2)	3.245(3)	163(4)

* Symmetry codes: $^{\#1}$ $1-x$, $1-y$, $1-z$ (**I**); $^{\#2}$ $-x$, $1-y$, $1-z$ (**II**); $^{\#3}$ $1/2-x$, $1/2+y$, $1/2-z$; $^{\#4}$ x, $-1+y$, z (**III**).

ligands. Such increased activity of the metal chelates can be explained on the basis of chelating theory [22].

In general, complexes **I** and **II** have similar antibacterial and antifungi activities against *Staphylococcus aureus*, *Escherichia coli*, and *Candida albicans*. However, complex **III** has obvious higher activities against the bacteria and fungi than complexes **I** and **II**. The same pattern is observed for the free Schiff bases. H_2L^c is more active than the other two. This phenomenon obvious indicates that the fluoro-substitute groups are essential for the biological activity. For *Staphylococcus aureus*, the activity of complex **III** is less than the control drug Tetracycline. But for *Escherichia coli* and *Candida albicans*, the complex has

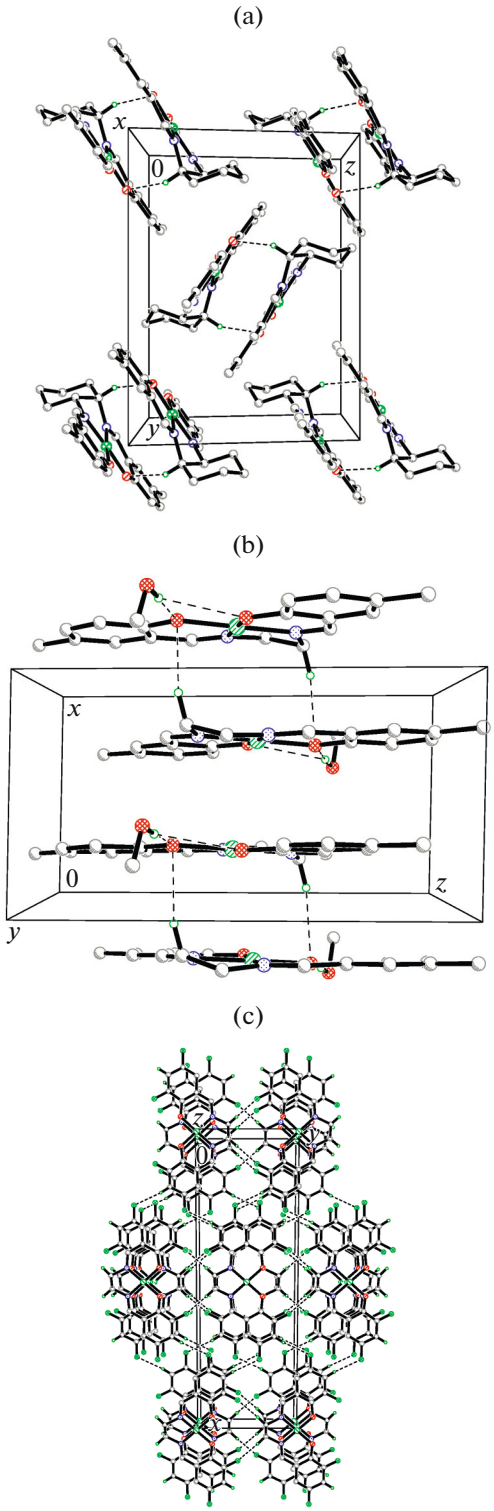

Fig. 2. Crystal structure of complexes **I** (a), **II** (b), **III** (c). Hydrogen bonds are drawn as dashed lines.

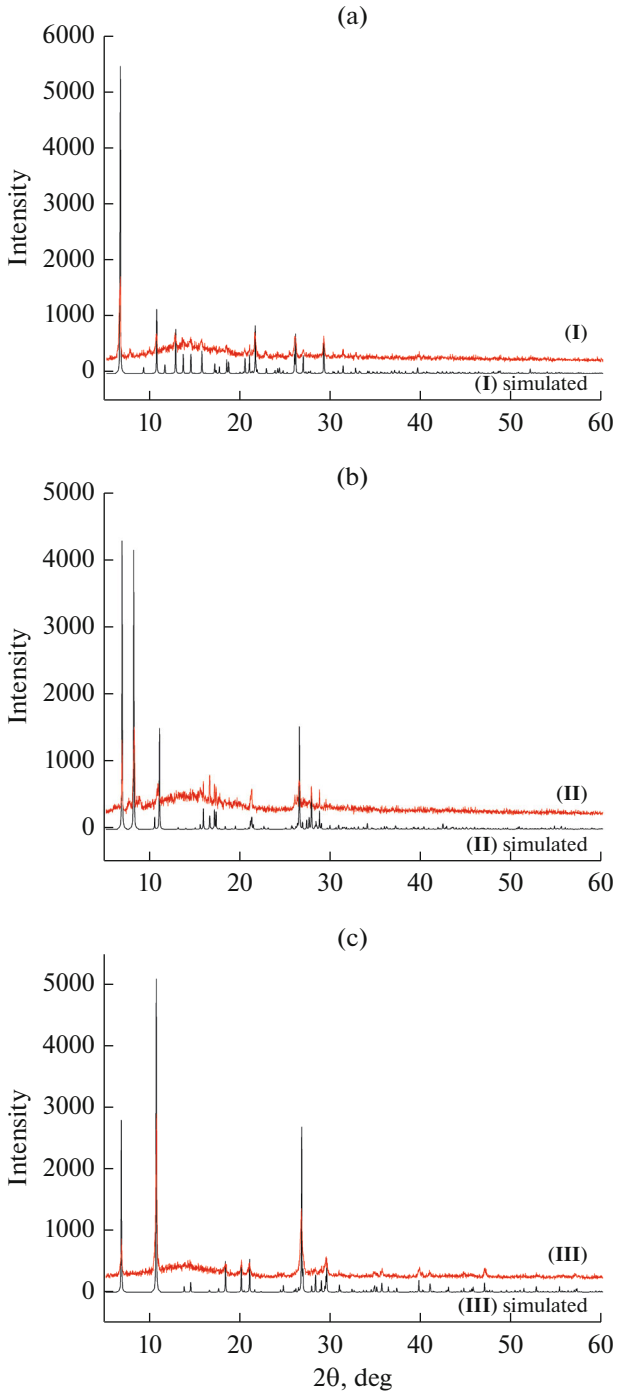

Fig. 3. Experimental and simulated powder XRD patterns of complexes **I** (a), **II** (b), **III** (c).

stronger activities than Tetracycline. Further work needs to be carried out to investigate the structure–activity relationship.

In summary, three nickel(II) complexes with bis-Schiff bases have been prepared and characterized. The crystal structures of the complexes were confirmed by XRD. The nickel atoms in the complexes are in square planar coordination. The biological test

Table 4. MIC values (μg/mL) for the antimicrobial activities of the tested compounds

Compound	*Staphylococcus aureus*	*Escherichia coli*	*Candida albicans*
H_2L^a	128	256	>1024
H_2L^b	128	256	>1024
H_2L^c	16	32	128
I	8	32	64
II	8	32	64
III	2	2	8
Tetracycline	0.30	2.15	>1024

shows that the complex with fluoro-substituted Schiff base ligand has effective activities against *Staphylococcus aureus*, *Escherichia coli*, and *Candida albicans*. Fluoro-subsituted groups in the Schiff bases may play important role in the biological processes.

FUNDING

This research was supported by the Top-class foundation of Pingdingshan University (nos. PXY-BSQD-2018006 and PXY-PYJJ-2018002).

REFERENCES

1. Liu, X. and Hamon, J.-R., *Coord. Chem. Rev.*, 2019, vol. 389, p. 94.
2. Khalf-Alla, P.A., Hassan, S.S., and Shoukry, M.M., *Inorg. Chim. Acta*, 2019, vol. 492, p. 192.
3. Crans, D., Koehn, J., Petry, S., et al., *Dalton Trans.*, 2019, vol. 48, no. 19, p. 6383.
4. Cifuentes-Vaca, O.L., Andrades-Lagos, J., Campanini-Salinas, J., et al., *Inorg. Chim. Acta*, 2019, vol. 489, p. 275.
5. Malik, M.A., Raza, M.K., Dar, O.A., et al., *Bioorg. Chem.*, 2019, vol. 87, p. 773.
6. Forouzandeh, F., Keypour, H., Zebarjadian, M.H., et al., *Polyhedron*, 2019, vol. 160, p. 238.
7. Yuan, C.X., Lu, L.P., Gao, X.L., et al., *J. Bio. Inorg. Chem.*, 2009, vol. 14, no. 6, p. 841.
8. Sonmez, M., Celebi, M., and Berber, I., *Eur. J. Med. Chem.*, 2010, vol. 45, no. 5, p. 1935.
9. Fekri, R., Salehi, M., Asadi, A., et al., *Inorg. Chim. Acta*, 2019, vol. 484, p. 245.
10. Kaczmarek, M.T., Zabiszak, M., Nowak, M., et al., *Coord. Chem. Rev.*, 2018, vol. 370, p. 42.
11. Zhang, M., Xian, D.-M., Li, H.-H., et al., *Aust. J. Chem.*, 2012, vol. 65, no. 4, p. 343.
12. *SMART and SAINT, Area Detector Control and Integration Software*, Madison: Bruker Analytical X-ray Instruments Inc., 1997.
13. Sheldrick, G.M., *SADABS, Program for Empirical Absorption Correction of Area Detector Data*, Göttingen: Univ. of Göttingen, 1997.
14. North, A.C.T., Phillips, D.C., and Mathews, F.S., *Acta Crystallogr., Sect. A*, 1968, vol. 24, no. 3, p. 351.
15. Sheldrick, G.M., *SHELXL-97, Program for the Refinement of Crystal Structures*, Göttingen: Univ. of Göttingen, 1997.
16. Mukherjee, P., Drew, M.G.B., and Ghosh, A., *Eur. J. Inorg. Chem.*, 2008, no. 21, p. 3372.
17. Cui, Y.M., Yan, W.X., Cai, Y.J., et al., *J. Coord. Chem.*, 2010, vol. 63, no. 21, p. 3706.
18. Siegler, M.A. and Lutz, M., *Cryst. Growth Des.*, 2009, vol. 9, no. 2, p. 1194.
19. Lal, R.A., Choudhury, S., Ahmed, A., et al., *J. Coord. Chem.*, 2009, vol. 62, no. 23, p. 3864.
20. Barry, A., Procedures and theoretical considerations for testing antimicrobial agents in agar media, in *Antibiotics in Laboratory Medicine*, Lorian V., Ed., Baltimore: Williams and Wilkins, 1991.
21. Rosu, T., Negoiu, M., Pasculescu, S., et al., *Eur. J. Med. Chem.*, 2010, vol. 45, no. 2, p. 774.
22. Searl, J.W., Smith, R.C., and Wyard, S., *J. Proc. Phys. Soc.*, 1961, vol. 78, no. 505, p. 1174.